BIOTIC AND ABIOTIC FORCING DURING THE TRANSITION TO MODERN GRASSLAND ECOSYSTEMS: EVOLUTIONARY AND ECOLOGICAL RESPONSES OF SMALL MAMMAL COMMUNITIES OVER THE LAST 5 MILLION YEARS

DAVID L. FOX[1], ROBERT A. MARTIN[2], ELIZABETH ROEPKE[3], ANNE C. FETROW[3], BRENDEN FISCHER-FEMAL[3], KEVIN T. UNO[4], KENA FOX-DOBBS[3], KATHRYN E. SNELL[5], ANDREW HAVELES[6,] and PRATIGYA J. POLISSAR[4]

[1]Department of Earth Sciences, University of Minnesota, Minneapolis, MN 55455 <dlfox@umn.edu>

[2]Department of Biological Sciences, Murray State University, Murray, KY 42071

[3]Department of Geology, University of Puget Sound, Tacoma, WA 98416

[4]Lamont-Doherty Earth Observatory, Columbia University, Palisades, NY 10964

[5]Department of Geological Sciences, University of Colorado, Boulder, CO 80309

[6]Department of Earth Sciences, University of Minnesota, Minneapolis, MN 55455

Abstract.—Understanding the origin of modern communities is a fundamental goal of ecology, but reconstructing communities with durations of 10^3–10^6 years requires data from the fossil record. Early Pliocene to latest Pleistocene faunas and sediments in the Meade Basin and modern soils and rodents from the same area are used to examine the role of environmental change in the emergence of the modern community. Paleoenvironmental proxies measured on modern surface soils and paleosols are described, and faunal dynamics of fossil rodents are discussed. Mean annual precipitation (MAP) was estimated from elemental concentrations and magnetic properties, and warm-season temperature and $\delta^{18}O$ of soil water was estimated using carbonate isotope paleothermometry on pedogenic nodules. MAP and temperature estimates from paleosols exhibit no short-term variability, no long-term trends, and generally bracket modern values. Estimated soil water $\delta^{18}O$ values increased through time, suggesting aridification played a role in the evolution of the regional grassland ecosystem. Carbon isotope analyses of biomarkers are used to examine the abundance of C_4 grasses, which suggest more C_4 biomass and more variability in C_4 biomass than carbonate proxies. Rodent species richness remained constant due to balanced rates of extinction and immigration, both of which show episodic spikes consistent with a balance between forcing mechanisms that result in equilibrium on long time scales. Overall, these results suggest that different mechanisms of faunal change may be acting at different time scales, although the stratigraphic resolution of paleoenvironmental proxies needs to be increased, and body size and dietary distributions of rodents need to be determined before which processes of change are most important can be decided.

INTRODUCTION

Identifying primary driving factors in the phylogenetic, morphological, and ecological evolution of communities over geological time is a fundamental problem in evolutionary biology and paleobiology. Various hypotheses have been suggested, sometimes lumped into either biotic or abiotic influences, commonly referred to respectively as "Red Queen" models after Van Valen (1973) and "Court Jester" models after Barnosky (2005), but these categories are not mutually exclusive and both probably play a role to some extent. For example, a Beringian corridor developing between Siberia and Alaska during a time of low sea level is certainly abiotic, but if it allows the immigration of species from the Old World that may be better adapted to North American ecosystems, then one could argue that competition is involved. Then again, perhaps the

In: *Earth-Life Transitions: Paleobiology in the Context of Earth System Evolution. The Paleontological Society Papers, Volume 21, P. David Polly, Jason J. Head, and David L. Fox (eds.). The Paleontological Society Short Course, October 31, 2015.*

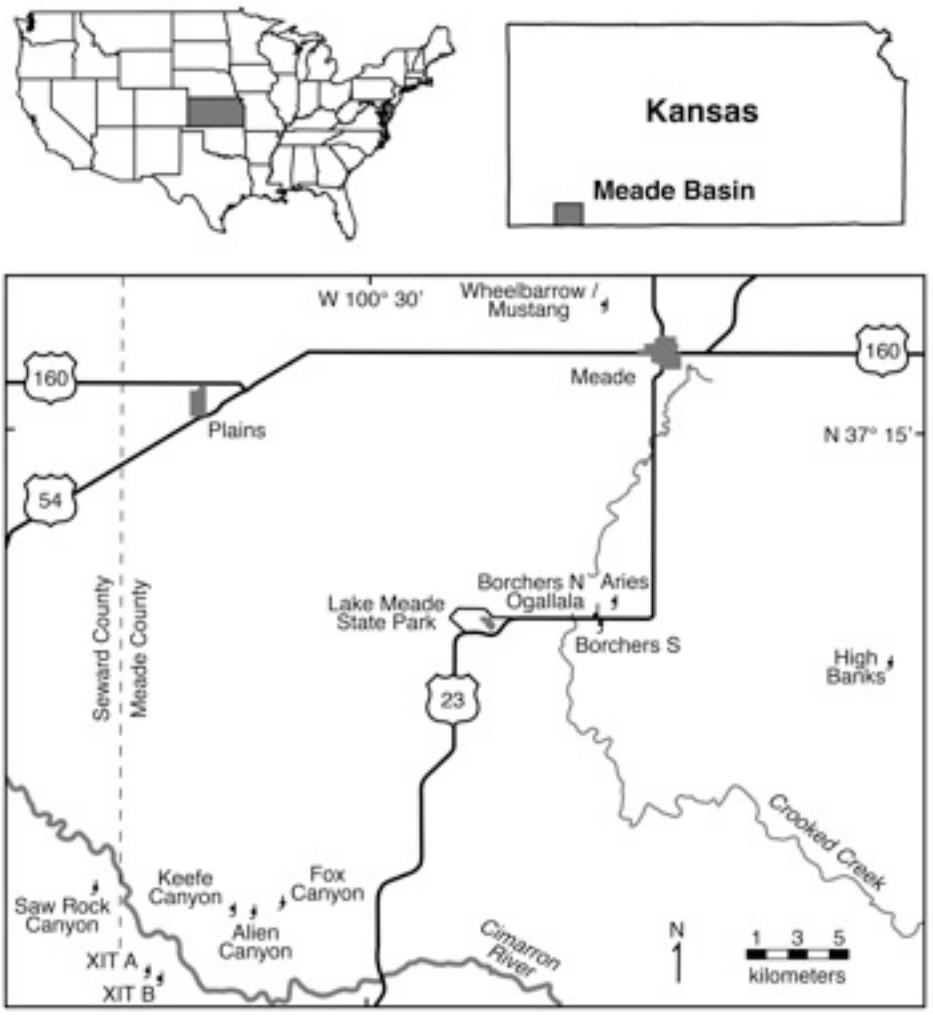

FIGURE *1*.—Map of the Meade Basin field area, Kansas, USA. Symbols indicate locations of important sections that produce rodent fossils discussed in the text. On the north side of the Cimarron River, symbols for some sections completely overlap and cannot be distinguished.

environment was changing to such an extent that the new immigrants found mostly empty North American niches as potential competitors, if present at all, were already on the verge of extinction. Under such a circumstance, the distinction between competition and environmentally driven extinction is ambiguous. It is noteworthy that despite the considerable time and effort made to develop competitive scenarios for community organization in the early days of theoretical ecology (Hutchinson, 1959; Jaeger, 1974), global competitive exclusion of one species by another has never been documented in nature. Competition surely plays an important role in determining momentary community function, but it may play a negligible or, at best, a 'coup de grace' role in global species extinctions. In this paper, we use the taxonomic composition and ecological structure of successive rodent communities in the Meade Basin of southwestern Kansas (Figure 1) to examine community turnover in the context of regional and global environmental changes. The primary goal is to test the hypothesis that environmental change drives rodent community turnover, rather than the biotic interactions among incumbent and immigrant species. If a relationship between environmental and community change can be identified, we can attempt to determine the tempo and mode of the influences of environmental change on community structure.

Equilibrium theory (MacArthur and Wilson, 1967) is also applicable to this study system. MacArthur and Wilson's (1967) model holds that an equilibrium number of species on ecological 'islands' is established due to the interplay of

immigration and extinction rates, the distance of islands (sinks) from continental biotas (sources), island size, and available niche space (habitat heterogeneity). Equilibrial systems need not be static and can exhibit stochastic behavior with pulses of increased immigration/extinction linked with more modest responses. One of the characteristics of the island biogeographic model is that the equilibrium number is maintained despite species turnover. Theoretically, a similar dynamic could develop over certain periods of time in a geographically proscribed continental ecosystem.

The Meade Basin is a northeast-southwest trending, ~50 km^2 depositional basin that stretches from the area of Meade, Kansas into the Oklahoma panhandle, and preserves well-exposed late Miocene to latest Pleistocene deposits (Fig. 1). The Meade Basin record is an ideal natural laboratory for testing hypotheses of faunal and ecological change in terrestrial ecosystems for several reasons.

First, the stratigraphy, geochronology, and biostratigraphy of the area (Fig. 2) are well understood (Hibbard and Taylor, 1960; Zakrzewski, 1975; Izett and Honey, 1995; Martin et al., 2000; Honey et al., 2005; Martin et al., 2008). The Pliocene and younger deposits have a long history of fossil collecting beginning with the pioneering screen-washing efforts of Claude Hibbard in the late 1930s that continued until his death in 1973. Work in the area was renewed by one of us (R. Martin) and collaborators with the inception of the Meade Basin Rodent Project (MBRP) in 1997, with the goals of generating a database of rodent species occurrences in the Meade Basin over the last 5 Myr, and using that database to test hypotheses of faunal and ecological change. Work on the MBRP over the last 18 years has led to revisions to the stratigraphy of the area, the relocation and recollection of many of Hibbard's classic localities, and the discovery of numerous new localities scattered stratigraphically throughout the original sequence of localities (Fig. 2).

Second, the species-level taxonomy throughout the Meade Basin sequence has now been sufficiently scrutinized and revised so that the database of species occurrences is suitable to begin testing evolutionary and ecological hypotheses. Included here is the current form of the database (Appendix); some minor revisions likely will occur as work on some clades of rodents is finished, but the database is close to complete at this point in terms of recognition of unique species-level taxa in most local faunas.

Third, the Meade sequence records the in-situ evolution of the modern rodent community in a limited geographical region over geological timescales (Fig. 3). Understanding the origin of modern communities is a fundamental goal of ecology, but reconstructing the history of communities that include species with stratigraphic durations on the scale of hundreds of thousands to millions of years—timescales over which geographic ranges can shift substantially—necessarily requires data from the fossil record. Similarly, inferences about the paleoecology of past communities are most robust when informed by data from both living and fossil populations of extant species. Despite the logical connections between ecology and paleoecology, relatively few studies have bridged the gaps in the characteristic observational timescales and methodologies of these disciplines to achieve a comprehensive view of the long-term evolution of specific modern communities. The 5-million year Meade Basin record is a system in which this can be done.

Finally, previous work as part of the overall MBRP has developed a detailed stable isotope record of pedogenic carbonates through the sequence (Fig. 3). The carbon isotope record indicates that the proportion of plants using the C_4 photosynthetic pathway (primarily warm growing-season grasses and some sedges) relative to those using the C_3 pathway (trees, shrubs, and cool growing-season grasses) was 0–10% during the late Miocene, ~40±20% throughout the Pliocene, and increased steadily during the early to Middle Pleistocene from ~50% to the characteristic modern abundance of ~80% (Fox et al., 2012a). The oxygen isotope record from these carbonates was interpreted as suggesting some combination of long-term cooling, increased soil moisture content, and/or increased recharge of soil water with winter precipitation (Fox et al., 2012b).

Currently, the MBRP is focused on addressing three related research questions:

1) Do long-term changes in local habitat or climate control taxonomic diversity dynamics? The existing local paleoenvironmental record based on paleosol carbonates (Fox et al., 2012a, b) provides an important but restricted picture of habitat composition and structure (abundance of C_4 grasses from $\delta^{13}C$ values) and an underdetermined measure of paleoclimate ($\delta^{18}O$ values). To address this question, we are

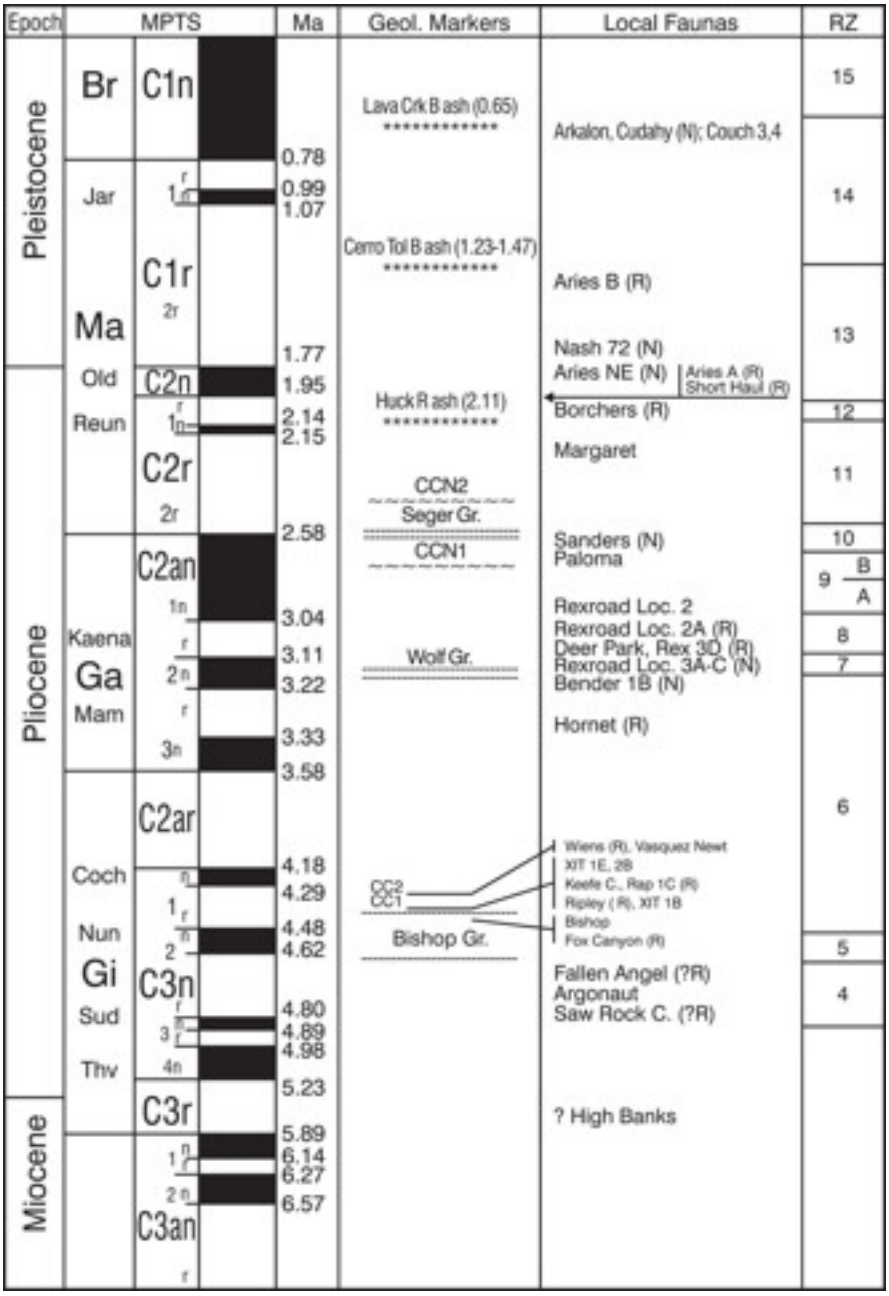

FIGURE *2*.—Stratigraphic relationships of Meade Basin local faunas. MPTS, magnetic polarity time scale; Ma, millions of years ago; C, Chron; r, reversed; n, normal; Br, Brunhes; Ma, Matuyama; Ga, Gauss; Gi, Gilbert; Jar, Jaramillo; Old, Olduvai; Reun, Reunion; Mam, Mammoth; Coch, Cochiti; Nun, Nunivak; Sud, Sidufjall; Thv, Thvera; Crk, Creek; Tol, Toledo; Huck R, Huckleberry Ridge; Gr., gravel; CC, calcium carbonate layer; (N) and (R), normal and reversed polarity; Rex, Rexroad; Rap, Raptor; C., Canyon; RZ, rodent zones of Martin (2003).

developing a comprehensive paleoenvironmental and paleoclimatic reconstruction through the Meade Basin sequence of local faunas using both well-established and relatively novel proxies: carbonate clumped isotope paleothermometry, δD and $\delta^{13}C$ values of leaf-wax *n*-alkanes in sediments, lignin phenols, $\delta^{13}C$ of bulk sedimentary organic matter, environmental rock magnetism, paleosol elemental geochemistry, and plant phytoliths. Ultimately, diversity dynamics in the rodent database will be compared to changes in environment and climate from these proxies.

2) Do ashfall events impact diversity dynamics or ecological structure of communities? The Pleistocene section in the Meade Basin includes three major ashfalls at 2.11 Ma

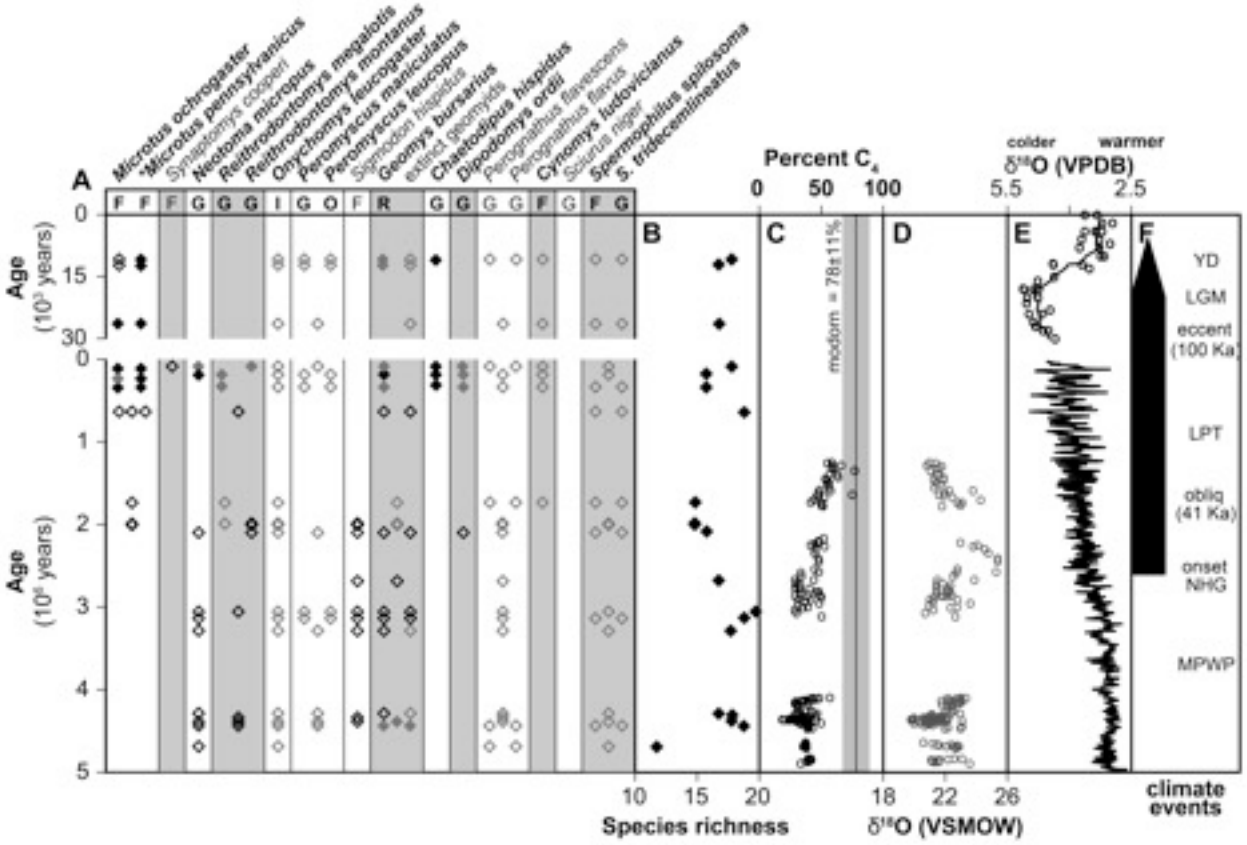

FIGURE 3.—Stratigraphic distribution of extant rodent species in the fossil record of the Meade Basin in relation to local and global environmental and climatic changes. A) Fossil occurrences of modern species and genera in 20 well-sampled Meade faunas. Closed black diamond=extant; closed grey diamond= cf. extant species; open black diamond=extinct; open grey diamond =extinct, identified as "sp."; trophic categories after Badgley and Fox (2000): F, folivore; G, granivore; R, roots; O, omnivore; I, invertebrates. B) Species richness by fauna (Martin et al., 2008); C) Percent C_4 biomass based on $\delta^{13}C$ values of Meade Basin paleosol carbonates; line and grey box indicate mean modern abundance for KS and OK (Fox et al., 2012a); D) $\delta^{18}O$ values of Meade Basin paleosol carbonates (Fox et al., 2012b); E) $\delta^{18}O$ of benthic foraminifera (Zachos et al., 2001); F) Global Plio–Pleistocene climatic events: Mid-Pliocene Warm Period (MPWP), Northern Hemisphere Glaciation (NHG), obliquity dominant (obliq), Late Pleistocene Transition(LPT), eccentricity dominated (eccent), Last Glacial Maximum (LGM), Younger Dryas (YD).

(Huckleberry Ridge), 1.47–1.24 Ma (Cerro Toledo B), and 0.64 Ma (Lava Creek) that deposited decimeters to meters of ash locally. Previously demonstrated taxonomic differences between the Borchers fauna from within and just above the Huckleberry Ridge Ash and stratigraphically higher local faunas suggest a role for catastrophic forcing of faunal change. To test this in greater detail, we are screen-washing sediments from short stratigraphic intervals above and below each ash in the Meade Basin to analyze the taxonomic and ecological structure of faunal samples before and after each ashfall.

3) How are immigrants accommodated in the ecological structure of the contemporary community in terms of body-size distributions and trophic structure? Immigrants that are ecologically similar to incumbents in terms of body size and/or diet could cause incumbents to shift their body size or diets relative to populations in earlier local faunas, indicating a response consistent with biotic controls on community structure, perhaps conforming to classic character displacement (Brown and Wilson, 1956). However, as shown by Martin et al. (2012), when size distributions of potential competitors were examined over long periods of time, even when one species expressed a change of size in the presence of another, competition was not always indicated. Nevertheless, rodent community organizational change will be examined by a) reconstructing body-size distributions for each local fauna by estimating mean body mass for each species using equations

based on regressions of tooth dimensions and body size in modern species, b) estimating diets of each species using carbon isotope analyses of tooth enamel and morphometric estimates of trophic category based on 3-D tooth crown morphology from high-resolution microCT scans, and c) translating body-size data into species and community energetic and life-history patterns (Martin, 1986).

The MBRP began to address these issues with new field work in May 2014, followed by lab work on the collected geological and paleontological samples. Describing all ongoing work is beyond the scope of this paper, so here, we summarize the initial paleoprecipitation estimates from chemical weathering indices and rock-magnetic properties of paleosols, paleotemperature estimates from carbonate clumped-isotope paleothermometry, and $\delta^{13}C$ values of leaf waxes. The current state of analyses of the diversity dynamics and body-size distributions from the rodent species database is described. Geological samples collected during fieldwork in June 2015 will increase the stratigraphic coverage of the data presented from the earliest Pliocene levels with fossil rodents (Saw Rock Canyon, Fig. 2) to the latest Pleistocene (Golliher B, Fig. 2), but these samples have not been analyzed yet for paleoenvironmental or paleoclimatic proxies.

PALEOCLIMATIC AND PALEOENVIRONMENTAL RECONSTRUCTION

Field sampling

Samples for paleoclimatic and paleoenvironmental proxy analyses were collected from outcrops (Fig. 4A) that included at least one local fauna to connect individual samples to the stratigraphic scheme for the Meade Basin (Honey et al., 2005; Martin et al., 2008; Fox et al., 2012a, b) and to individual local faunas. Samples were collected from measured sections after trenching outcrops on steep slopes to depths of ~20–70 cm perpendicular to the outcrop face to reduce effects of surficial weathering on the materials analyzed. Samples were generally collected at ≥10-cm intervals within discrete beds that exhibited evidence of pedogenesis prior to burial (e.g., disrupted bedding, drab-haloed root traces, calcareous rhizoconcretions, slickensides, abundant clay, carbonate nodules, and/or gradational transitions in color and structure), or at larger intervals through sections with sands and coarser beds that are not suitable for our proxy analyses (i.e., channel deposits with no pedogenesis), or that lack carbonate. Sample spacing within outcrops ranged from 3 cm to 277 cm (Fig. 4A). At each sampling level, separate samples were collected for bulk elemental analysis, rock magnetic analysis, and phytolith extraction; carbonate clumped-isotope (i.e., Δ_{47}) analysis (where reliably authigenic pedogenic carbonate was present); bulk organic matter carbon isotope analysis; and compound-specific carbon and hydrogen isotope analysis of leaf-wax n-alkanes and n-alkanoic acids.

Paleoprecipitation

Background.—The degree of chemical weathering of silicates and iron oxides in active surface soils is sensitive to local mean annual precipitation (Sheldon et al., 2002; Retallack, 2007; Geiss et al., 2008; Sheldon and Tabor, 2009; Heslop and Roberts 2013). Two well-established paleoprecipitation proxies based on elemental ratios in pedogenically altered sediments were used for these analyses. The first, the Chemical Index of Alteration without Potassium (CIA-K; see discussion in Sheldon and Tabor, 2009), is intended to express the extent of chemical weathering in a soil as a function of feldspar weathering while accounting for alterations in concentration of potassium through interactions with fluids and clay formation. CIA-K is calculated for elemental concentrations converted to moles as:

$$CIA-K = 100 \times \frac{Al2O3}{Al2O3 + CaO + Na2O} \quad \text{Eq. (1)}$$

Sheldon et al. (2002) showed that CIA-K for modern soils correlates with local mean annual precipitation (MAP, in mm/yr) and can be used to predict MAP using the expression:

$$MAP = 221e^{0.0197(CIA-K)} \quad \text{Eq. (2)}$$

The Mollisol-specific (hereafter referred to as C index) MAP proxy, also proposed by Sheldon et al. (2002), is specific to B horizons of mollisols or grassland soils:

$$MAP = -130.9 \ln(C) + 467 \quad \text{Eq. (3)}$$

where C is the ratio of Ca to Al, again expressed in moles. For discussion of these proxies, see

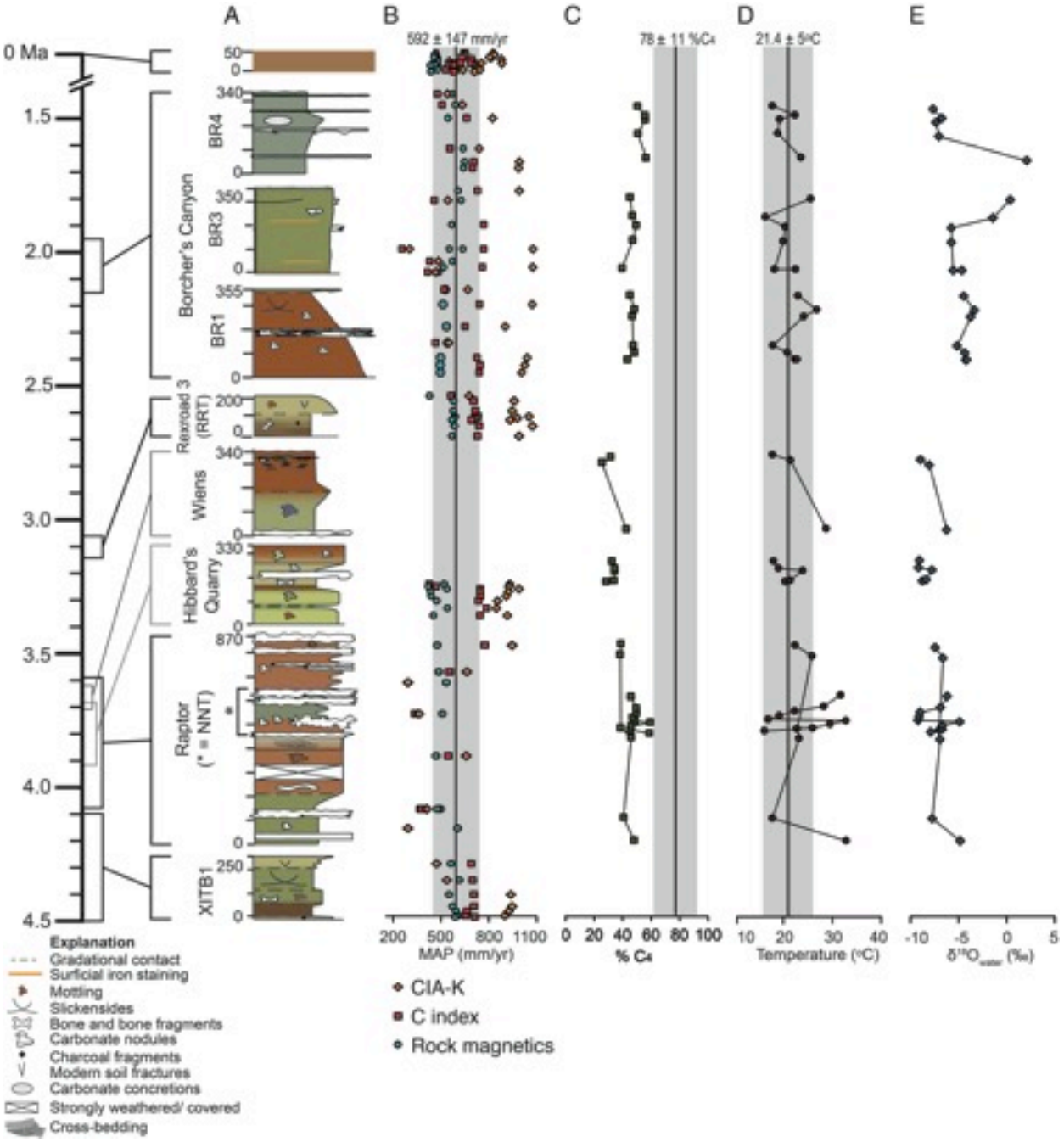

FIGURE *4*.—Lithostratigraphy of measured sections sampled in the Meade Basin during fieldwork in 2014, and paleoclimate estimates from proxy analyses of those samples: A) Lithostratigraphy of individual measured sections with age assignments based on associated rodent local faunas in Fig. 2; B) Estimated mean annual precipitation (MAP) in mm/yr from CIA-K, C index, and rock magnetic properties; vertical line indicates modern MAP for Meade and grey box indicates 1 standard deviation around mean value; C) Percent C_4 calculated as described in the text from $\delta^{13}C$ values measured during carbonate clumped-isotope analyses; vertical line indicates mean modern percent C_4 biomass in Kansas and the Oklahoma panhandle, and grey box indicates 1 standard deviation around the mean value, based on Fox et al. (2012a); D) Paleotemperatures calculated from Δ_{47} values as described in the text; vertical line indicates mean warm season (June–August) temperature in Meade, KS; grey box indicates 1 standard deviation around the mean value; E) calculated soil water $\delta^{18}O$ values based on measured carbonate $\delta^{18}O$ values and estimated soil temperatures in (D).

review by Sheldon and Tabor (2009).

A proxy for MAP based on rock magnetic properties of paleosols developed by Geiss et al. (2008) specifically for Holocene soils developed on loess was also used. This proxy has not been applied to older paleosols or those developed on other parent materials. Sediments in the Meade Basin are dominantly fluvial with limited or no evidence for aeolian deposition in most sections; we applied this proxy to compare to the elemental indices because it is relatively easy and quick to measure. The rock magnetic proxy is based on the ratio of the anhysteretic remanent magnetization (ARM) to the isothermal remanent magnetization (IRM), which is sensitive to the remanence of pedogenic maghemite. This ratio is related to MAP by the expression:

$$MAP = 363.736 + \left[40.2133 \times \left(\frac{ARM/_{50\mu T}}{IRM}\right) \times 10^4\right] \quad \text{Eq. (4)}$$

The goal in using this proxy is to compare estimates from magnetic properties to those based on elemental rations to determine how this proxy behaves for paleosols that developed on parent materials other than loess.

Methods.—Elemental concentrations and rock magnetic properties were measured from 67 bulk sediment samples from nine measured sections that range in age from early Pliocene (ca. 4 Ma) to mid-Pleistocene (ca. 1 Ma), and from three modern surface-soil pits. Three stratigraphically successive sections were measured and sampled in the early Pleistocene Borchers Badlands section (BR1, 3, 4 in Fig. 4A). For elemental concentrations, samples were dried at 60°C overnight prior to grinding in a SPEX 800-115 ball mill for 10–15 minutes. Samples were then digested in HCl, HF, HNO_3, and HBO_4 in a CEM Discover Explorer microwave digester. Samples were analyzed with a Thermo Scientific iCAP 6000 interfaced with a CETAC ASX-520 Auto-Sampler in the Aqueous Geochemistry Lab at the University of Minnesota. Reported values are averages of 15 analyses per sample, ± 1 standard deviation. For rock magnetic properties, pellets ~2 cm on a side were cut from each sample, glued into small plastic boxes, and used for susceptibility, ARM, and IRM measurements in the Institute for Rock Magnetism at the University of Minnesota. Magnetic susceptibility was measured at 465 Hz and 4650 Hz to determine the amount of superparamagnetic material in the sample. Reported values are averages of five measurements at different orientations. ARM measurements were determined under a bias field of 50 mT.

Results and discussion.—Modern mean annual precipitation as rain for Meade, KS, is 545±132 mm/yr, and mean annual snowfall is 471±239 mm/yr (Meade station NCDC Summary of the Day, www.ncdc.noaa.gov/oa/ncdc.html). Assuming ~10% snow water equivalent yields an effective modern MAP for the area of 592 mm/yr. For the three surface soils, the elemental proxies predict generally higher MAP than observed, with estimates ranging from 550 mm/y to 828 mm/y (Fig. 4B). Estimates from CIA-K for all three modern soils are considerably higher than the measured modern value (653–828 mm/yr); estimates from the C index range from 549 mm/y to 651 mm/yr, so for one modern soil, the C index provides an accurate estimate of modern MAP. The estimates from the magnetic proxy for pedogenic maghemite production are generally lower than modern MAP, and range from 480 mm/y to 504 mm/yr. The higher estimates for modern soils could result from the soils forming under wetter conditions earlier in the Holocene, but given that the different proxies yield different deviations from modern MAP, it is also possible that one or more of the soils is not in geochemical equilibrium with climate yet, and therefore the proxies could be recording parent material signatures. Notably, each proxy has the same order of soils from highest to lowest estimated MAP regardless of absolute value.

For the paleosols, MAP estimates from CIA-K are generally higher than those for the C index, which are generally higher than those for ARM/IRM (Fig. 4B), as is the case for the modern soils. Estimates from CIA-K vary through the sections from 293–1165 mm/yr, with a mean of 790±225 mm/yr. MAP estimates by the C index range from 238-785mm/yr, with a mean of 612±142 mm/yr. MAP estimates from the magnetic proxy range from 423–650 mm/yr, with a mean of 526±62 mm/yr. With only a few exceptions, through most of the Meade sequence, the estimates from CIA-K are consistently higher than modern MAP, the estimates from the C index are close to the modern value, and the estimates from ARM/IRM are lower than modern MAP for splits of the same sample. For the Rexroad Loc. 3 samples, the estimates from ARM/IRM are just below the modern value, and those for CIA-K and the C

index are both above the modern value, but the sediments at Rexroad Loc. 3 show little or no evidence of extensive pedogenesis, so this is likely not a true climate signal. At the top of the Borchers sequence, some of the samples in the BR4 section have estimates for all three proxies that are higher than the modern value. In general, neither individual sections nor the entire sequence suggest strong changes stratigraphically in MAP throughout the Meade sequence. Given that the estimates from C indices for the modern surface soils were closest to modern MAP, it seems that MAP did not vary substantially from modern in southwest Kansas over the last 4 Ma, at least within the resolution of sampling so far.

Carbonate Clumped-Isotope (Δ_{47}) Thermometry

Background.—Carbonate forms naturally in a variety of settings and is part of many common minerals, including calcite, dolomite, aragonite, and siderite. During the precipitation process, 'clumping" of heavy isotopes, ^{18}O-^{13}C, in carbonate ions, becomes more pronounced as the temperature decreases during mineral formation (Eiler and Schauble, 2004; Ghosh et al., 2006; Eiler, 2007; Huntington et al., 2009; Quade et al., 2013). This preferential 'clumping' of the heavier and rarer isotopes into the same molecule is thermodynamically favored at cooler temperatures, rather than a random distribution of isotopes (Eiler and Schauble, 2004; Wang et al., 2004; Ghosh et al., 2006;). A measurable form of these isotopologues can be produced by digestion of carbonate powder in phosphoric acid to produce CO_2 (Swart et al., 1991). The "clumped" isotopologue of this evolved CO_2 (^{18}O-^{13}C-^{16}O) has a molecular mass of 47 (Ghosh et al., 2006), and is the most abundant of the heavy-substituted isotopologues (Eiler and Schauble, 2004; Eiler, 2007). The inverse relationship between 'clumping' and temperature of carbonate formation is described by Ghosh et al. (2006), and can be used as a paleothermometer. The abundance of mass 47 is expressed as the ratio of measured mass 47 to measured mass 44 ($R^{47}_{sample} = M^{47}_{sample}/ M^{44}_{sample}$) compared to the expected R^{47} value for a stochastic distribution of ^{13}C and ^{18}O isotopes among CO_2 molecules (Eiler and Schauble, 2004; Eiler, 2007):

$$\Delta_{47} = \left(\frac{R^{47}_{sample}}{R^{47}_{Stochastic}} - 1\right) * 1000 \qquad \text{Eq. (5).}$$

Along with Δ_{47} temperature estimates, carbon ($\delta^{13}C$) and oxygen ($\delta^{18}O$) isotope values were determined for each carbonate sample. $\delta^{18}O$ of the water ($\delta^{18}O_w$) from which the mineral precipitated was calculated from the Δ_{47} temperature estimate and the $\delta^{18}O$ of the carbonate ($\delta^{18}O_c$). Carbon and oxygen stable isotope ratios are reported using delta notation, $\delta = \left[\frac{R_{sample}}{R_{standard}} - 1\right] * 1000$, where R is the ratio of the heavy to light isotope of the sample or standard and expressed on a permil scale (‰), relative to the Vienna Peedee Belemnite (VPDB) standard composition and Standard Mean Ocean Water (SMOW), respectively. From these analyses, we also calculated weight percent carbonate as a means to check that carbonates likely formed through pedogenesis, as well-developed paleosol carbonate nodules tend to be >50% carbonate, and samples with <50% carbonate may be the product of multiple stages of carbonate cementation and thus may not result from soil processes alone.

Methods.—Three to nine Stage II carbonate nodules or chunks of Stage III calcretes were analyzed per section, and tested for differences in both means and variances of paleotemperature estimates among sections. Carbonate nodules were cut along the longest axis using a rock saw and the cut surfaces were polished using a combination of polishing wheel, sand paper, and polishing glass with varying sizes of grit. The cut faces of most samples appeared homogenous, with no evidence for diagenesis, such as secondary mineral precipitation or recrystallized sections (e.g. large crystals or veins). Powder was carefully drilled only from nodule regions with no diagenetic indicators. From the polished faces, samples were taken from small areas with a dental drill under a binocular microscope to a maximum of 1–2 mm in depth. Sample powders were then ground with a mortar and pestle to homogenize the sample.

Approximately 10–12 mg of each powdered sample was weighed into an individual silver capsule and loaded into a sample carousel fitted to a semi-automated CO_2 gas generation and cleaning system (Huntington et al., 2009; Passey et al., 2010). In this system, carbonate samples and carbonate standards are digested in a bath of phosphoric acid held at 90° C, yielding CO_2 gas. The CO_2 gas, as well as heated gas standards that are prepared beforehand, are cryogenically purified by passing through traps at

approximately -60°C to remove water, and a poropak-filled gas chromatograph column held at -20°C to remove possible contaminants that have the same molecular masses as the CO_2 isotopologues of interest (masses 44, 45, 46, 47). Carbonate $\delta^{18}O$ values ($\delta^{18}O_C$) were calculated using the acid digestion fractionation factor of 1.000821 (Swart et al., 1991). Thirteen samples out of 44 showed excess mass 48, which is monitored as an indicator of sample purity; these mass 48 excesses may have been the result of incomplete cleaning of hydrocarbons or halocarbons that can produce potential interference with the Δ_{47} values (Ghosh et al., 2006; Huntington et al., 2009; Affek, 2012;).

Each CO_2 gas sample was analyzed 5–8 times on a modified Finnigan MAT 253 isotope ratio mass spectrometer at the California Institute of Technology; each of these acquisitions included 7–10 cycles of sample and reference gas peak determinations with 8-second peak integration times. The average isotope ratios from the 5–8 acquisitions were used to determine the uncorrected Δ_{47} values ($\Delta_{47,\ unc}$) and associated $\delta^{13}C$ and $\delta^{18}O$ values. Values for $\Delta_{47,\ unc}$ were corrected ($\Delta_{47,corr}$) for non-linearity effects in the mass spectrometer using a heated gas line generated from CO_2 gases heated to 1000°C. Changes in the heated gas line were corrected to instrument conditions during the determination of the original Δ_{47}-temperature calibration using a stretching factor, following the procedure discussed in Huntington et al. (2009) and Passey et al. (2010). For individual gas $\Delta_{47,\ unc}$ values analytical precision ranged from 0.0049‰ to 0.0163‰ (one standard error of the mean (1 s.e.)). Uncertainties for $\Delta_{47,corr}$ values in the data set range from 0.0077‰ to 0.0284‰, which includes error associated with the heated gas line in addition to the analytical uncertainties of the sample.

Heated gases and gases held at 25° C for equilibration with deionized water were used to create a transfer function that converted the "in-house" $\Delta_{47,\ unc}$ values to the Absolute Reference Frame (ARF). Two carbonate standards, CIT Carrara marble and TV03, were also analyzed to monitor instrument accuracy and precision during analysis. From the converted sample Δ_{47} values, temperatures were calculated using the revised calibration from Ghosh et al. (2006) that was converted to the ARF. Values of Δ_{47} from the standard carbonates were converted using the original conversion calculator reported in Ghosh et al. (2006). These two temperature conversions, which produce similar results, were then averaged to produce the temperature estimates presented in this study.

Results and discussion.—Weight percent carbonate ($wt\%_{carb}$) calculations were used to help to assess the likelihood that samples formed from soil processes, and thus that the temperature values reflect soil temperature. The majority of the samples analyzed have relatively high $wt\%_{carb}$ values for paleosol carbonate nodules. The $wt\%_{carb}$ values ranged from 36% to 91% with a mean of 72%, and the $wt\%_{carb}$ exhibits no obvious relationships with $\delta^{13}C$ values, Δ_{47} temperature estimates, or calculated $\delta^{18}O_{water}$ values. Together, these results suggest that the carbonate formed from soil processes and not a secondary fluid source (Snell et al., 2013). Further assessment of the fidelity of the record will be made from petrographic studies of the samples, which are currently ongoing.

Through the sampled sections, $\delta^{13}C$ values range from -6.7‰ to 2.0‰, with similar variance within sections, and generally, $\delta^{13}C$ values increase up-section, as previously demonstrated from independent samples through the same sections for conventional carbonate stable-isotope analyses (Fox and Koch, 2003, 2004; Martin et al., 2008; Fox et al., 2012a). The $\delta^{13}C$ values for the top samples in the Wiens section are anomalous, and may reflect local paleoenvironmental differences, such as vegetation heterogeneity, soil depth, or differences in carbon cycling between depositional environments. The linear mixing model described by Fox et al. (2012a) was used to convert $\delta^{13}C$ values to estimates of the percent C_4 plant biomass on the landscape. Percent C_4 increased from approximately 28% at 4.5 Ma to 60% at 1.8 Ma (Fig. 4C). The modern percent C_4 estimate for the Meade Basin is 78% ± 11% (Fox et al., 2012a). This percent C_4 record is in good agreement with the estimates reported by Fox et al (2012a) (Fig. 3).

Average paleotemperature estimates among sections ranged from 17° C to 24° C, with no systematic change through time (Fig. 4D); for reference, the modern mean annual and warm season temperatures for Meade, KS, are 14° C and 24° C, respectively (Fox et al., 2012b). There were differences in the variability of paleotemperature estimates within each section, and the standard deviations ranged from 1.3° C to 2.6° C. Within-section variability of temperature

estimates may result from a number of factors. First, temperature estimates derived from soil carbonate nodules often show a warm-season bias due to preferential formation of soil carbonate in summer months and/or during warm, dry conditions with low levels of soil CO_2 (Breecker et al., 2009; Passey et al., 2010; Quade et al., 2013; Hough et al., 2014). Thus, while we infer that these temperature estimates largely reflect summer temperatures, changes in the season of formation can introduce potential variability. Second, clumped isotope temperature estimates can be influenced by the amount of solar heating at the soil surface, which in turn is controlled by vegetation and shading (Hough et al., 2014). Third, as discussed in Quade et al. (2013), the depth of nodule formation in the soil may also have a significant impact on the Δ_{47} temperature estimates. At greater depths, soil temperatures are less affected by seasonal and diurnal cycles.

For most of these sections, some combination of these factors likely explains the observed variance in temperature estimates. We identified one section (NNT1) with a paleotemperature record that may reflect the variation in temperature that occurs due to depth of carbonate nodule formation along a soil profile. The oscillations in temperature estimates at NNT1 appear to reflect nodules formed along two stacked soil profiles. Recognition of the influence of these processes on Δ_{47} temperatures in soils is still relatively recent, and approaches have not yet been developed for how to best account for these effects in paleoclimate records derived from paleosol carbonates. The recognition of a temperature profile with depth in our samples is promising for further development of methods to account for this variability in paleoclimate records.

Calculated $\delta^{18}O_w$ values for paleosols increased steadily through time, except for an isolated positive excursion in the youngest sections sampled (BR3 and BR4). Average section $\delta^{18}O_w$ values ranged from -9.1‰ to 2.3‰ (Fig. 4E). Higher $\delta^{18}O_{water}$ values suggest the effect of evaporation on nodule carbonate source water, which may be a product of increased aridity. Soil depth will be an important factor to consider for this record as well because evaporation rates are likely to be higher for samples from shallower depths in the soil profile. In addition to recording potential changes in relative humidity through time, the increase in $\delta^{18}O_{water}$ values may also reflect the onset of global continental glaciation (Fox et al., 2012b) increasing the $\delta^{18}O$ of source waters by preferential storage of water with excess ^{16}O in continental ice sheets.

Compound-specific carbon isotope analysis of leaf wax *n*-alkanes

Background.—Plants produce waxes to protect leaf tissue from abrasion by dust, attack by insects and fungi, and water loss from the leaf surface. These waxes are made up of a variety of organic compounds that include *n*-alkanes and both free and esterified *n*-alkanoic acids and *n*-alcohols (Eglinton and Hamilton, 1967). The carbon isotopic composition of plant waxes reflects plant photosynthetic pathways and therefore records ecosystem vegetative structure in terms of the relative abundances of C_3 and C_4 plants. *n*-Alkanoic acids from C_3 plants have $\delta^{13}C$ values ranging from ~ -40‰ to -28‰, whereas C_4 plants range from -24‰ to -18‰. Within the last 25 years, development of analytical methods has enabled isotopic measurement for carbon isotopes of individual molecules by combining gas chromatography, combustion, and gas source isotope ratio mass spectrometry (Hayes et al., 1990; Burgoyne and Hayes, 1998).

Plant waxes are commonly preserved in sedimentary organic matter, where their resistance to diagenetic alteration and isotope exchange makes them an excellent geochemical proxy for vegetation and hydrologic studies in the geologic record (Freeman and Colarusso, 2001; Smith et al., 2007; Polissar et al., 2009). Numerous studies have utilized plant wax carbon isotopes from marine and lacustrine sediments ranging in age from Holocene to 35 Ma to reconstruct paleovegetation (Castañeda et al., 2009; Tipple and Pagani, 2010; Feakins et al., 2013). In the Meade Basin, we extend the application of isotopic analysis of *n*-alkanoic acids to paleosol, alluvial, fluvial, and pond sedimentary archives.

Methods.—Approximately 250 g to 500 g of sample for leaf-wax analyses were collected at each sampling level in each trench onto aluminum foil, and the same three modern soils were analyzed for paleoprecipitation proxies. Care was taken to avoid sampling modern roots or near areas where modern soil filled cracks in Neogene sediments. At each sampling level, both sediment matrix and carbonate nodules (stage II) or calcrete (stage III) samples were collected for analysis to compare the isotopic signal in bulk sedimentary organic matter to that occluded in carbonates. In the lab, the outer surface of indurated samples

was cleaned with a Dremel rotary tool to remove possible modern contamination by *n*-alkyl lipids. Samples were then wrapped in foil and crushed with an organic solvent-rinsed hammer into 1–3 cm sized pieces, placed in ashed jars, and freeze-dried overnight. Sample pieces were then crushed to a powder in a solvent-rinsed mortar and pestle. Between samples, the mortar and pestles were washed, rinsed with DI water, and solvent-rinsed with methanol and DCM.

Lipids were extracted from powdered samples with organic solvents (9:1 DCM: methanol) using an Accelerated Solvent Extractor (ASE) in batches of ~65 g of sample packed into 66 ml extraction cells. Extractions included four 10-minute static cycles at 100° C. The total lipid extract (TLE) was treated with sodium sulfate to remove water if was present. Less than 20% of samples required sodium sulfate treatment. The TLE was separated by solid-phase extraction on flash silica-gel columns (~1g Si-gel) where the aliphatic fraction (F1) was eluted with 4 ml of hexane, the ketone and ester fraction (F2) eluted with DCM, and the polar fraction (F3) with methanol. The F3 fraction was passed through an amino-propyl column (~0.5 g) where the neutral, acid (A), and polar fractions were eluted with 4ml of 2:1 DCM: isopropynol, 4% acetic acid in diethyl ether, and methanol, respectively. Carboxylic acids in the F3_A fraction were methylated (Me) with acidic methanol at 60° C for 4 to 12 hours, yielding fatty acid methyl esters. *n*-Alkanoic acids in the F3_A_Me fractions were isolated from hydroxy acids using a flash silica-gel column, where the F2 fraction contained the isolated *n*-alkanoic acids.

n-Alkanoic acids of Neogene sediments and modern soil samples were quantified and characterized on an Agilent gas chromatograph mass selective detector (GC-MSD) and flame ionization detector (FID). One microliter of sample in 100 µl of hexane was injected into a PTV injector at 60° C (0.1 min hold) ramped to 320°C at 900°C/min. Initial oven temperature was set at 60° C (1.5 min hold) and ramped to 150° C at 15° C/min, then to 320° C at 4° C/min. A splitter downstream of a DB-5 column (30 m length, 250 um ID) split He flow to the MSD and FID. Compound identification was done with mass spectra data, and quantification was done using FID peak areas. *n*-Alkyl lipid concentrations were calculated based on the peak area of known concentrations of the internal standard added to the TLE (cis-11-eicosenoic acid).

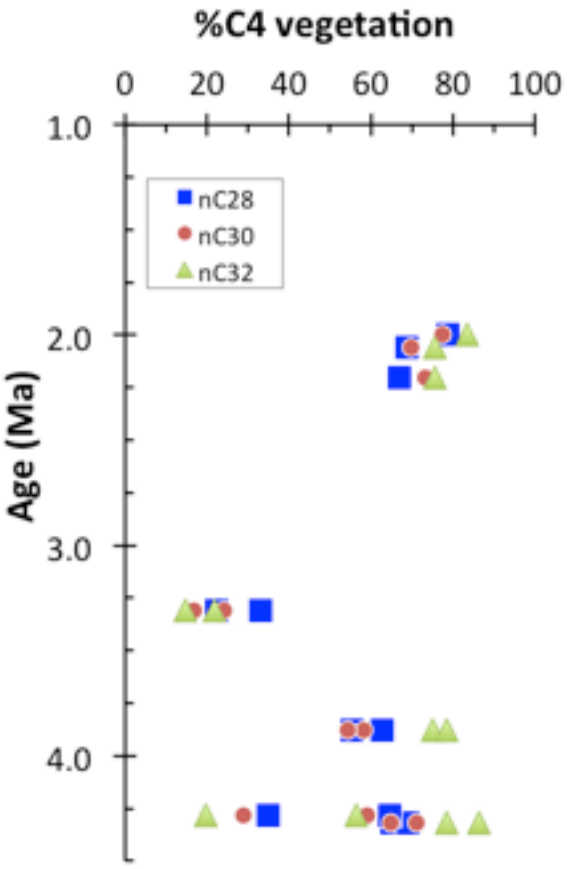

FIGURE 5.—Percent C_4 vegetation from $\delta^{13}C$ values of *n*-alkanoic acid homologues nC28, nC30, and nC32 are plotted vs. Age (Ma). Meade Basin terrestrial sediments include paleosols, alluvium, fluvial deposits.

Carbon isotope ratios from even-numbered *n*-alkanoic acids were analyzed using GC coupled to a Thermo Delta V isotope ratio mass spectrometer (IRMS) through a combustion interface at the Lamont Doherty Earth Observatory of Columbia University (LDEO) Stable Isotope Lab. All sample injections were interspersed with A4, A5, or F8 isotopic standards (obtained from Arndt Schimmelmann, Univ. of Indiana), which were used for correction of carbon isotope values. *n*-Alkanoic acid values were corrected using a mass-balance equation and the measured $\delta^{13}C$ value of the methanol used for methylation.

n-Alkanoic acid $\delta^{13}C$ values are reported as percent C_4 vegetation (%C_4) on the landscape, with end-member *n*-alkanoic acids $\delta^{13}C$ values for C_3 and C_4 vegetation of ~ -35‰ and -20‰. The

TABLE *1*.—$\delta^{13}C$ and %C4 data from *n*-alkanoic acids in Meade Basin sediments.

					$\delta^{13}C$ (per mil, VPDB)			%C4		
Sample ID	Site	Level (local datum, cm)	Approx. Age (Ma)	NALMA	nC28	nC30	nC32	nC28	nC30	nC32
MB140524.BR4.2 80.08-GCM	Borchers	280	2	Irvingtonian	-23.0	-23.3	-22.4	78.9	77.4	83.4
MB140524.BR3.2 00.06-GCM	Borchers	200	2.06	L Blancan	-24.4	-24.2	-23.3	68.8	69.8	75.7
MB140523.BR1.2 95.03-GCM	Borchers	295	2.2	L Blancan	-24.6	-23.7	-23.3	66.9	73.4	75.7
MB140526.RRT1. 90.05-GCM	Rex Rd 3	90	3.31	M Blancan	-31.3	-32.1	-32.4	22.3	16.8	14.7
MB140526.RRT1. 50.03-GCM	Rex Rd 3	50	3.31	M Blancan	-29.7	-31.0	-31.4	33.0	24.2	21.7
MB140525.RP1.1 95.06-GCM	Raptor	195	3.88	E Blancan	-25.1	-25.8	-23.3	62.8	58.2	75.0
MB140525.RP2.1 95.02-GCM	Raptor	195	3.88	E Blancan	-26.3	-26.4	-22.8	55.3	54.4	78.5
MB140522.XITB 1.40.04-GCM	XIT B	40	4.28	E Blancan	-24.9	-25.7	-26.1	64.5	59.0	56.6
MB140522.XITB 1.N05.03-GCM	XIT B	-5	4.28	E Blancan	-29.3	-30.2	-31.6	34.9	28.8	19.7
MB140521.HQ1.1 50.09-GCM	Keefe Quarry	150	4.32	E Blancan	-24.8	-24.8	-22.8	65.1	64.8	78.5
MB140521.HQ2.1 50.01-GCM	Keefe Quarry	150	4.32	E Blancan	-24.2	-23.9	-21.6	69.0	71.2	86.3
							min	22.3	16.8	14.7
							max	78.9	77.4	86.3
							mean	56.5	54.4	60.5

end-member values varied by 0.3‰ depending on the $\delta^{13}C$ value used for atmospheric CO_2, which ranged from -6.2‰ to -5.9‰ during the time interval studied. A two end-member mixing model was used to calculate $\%C_4$ using the following equation: $\%C_{4\ sample} = [(\delta^{13}C_{sample} - \delta^{13}C_{C3})/(\delta^{13}C_{C4} - \delta^{13}C_{C3})] \times 100$, where $\delta^{13}C_{C3}$ and $\delta^{13}C_{C4}$ are end member values.

Results and discussion.—Carbon isotope data from *n*-alkanoic acids in 11 Meade Basin samples are presented in Fig. 5 and Table 1. Data are reported as percent C_4 vegetation ($\%C_4$) on the landscape. Three homologues, C28, C30, and C32 are reported. The mean, minimum, and maximum $\%C_4$ values for each homologue are presented in Table 1, along with corresponding $\delta^{13}C$ values. The largest range of $\%C_4$ values is 71.6% in the C32 homologue, where the minimum, maximum, and mean are 14.7%, 86.3%, and 60.5%, respectively. The ranges for the C28 and C30 homologues are slightly smaller but similar. There are no apparent trends in vegetation over this interval.

The 15% to 86% range of C_4 vegetation calculated from the C32 homologue $\delta^{13}C$ data is greater than the 20% to 58% range calculated from soil carbonate $\delta^{13}C$ data spanning the same interval (early Blancan to early Irvingtonian, or ~4.3 to 2 Ma) in the basin (Fox et al., 2012a), as well as the range calculated from carbonates analyzed for carbonate clumped-isotope paleothermometry discussed above. The mean plant-wax $\%C_4$ values of 56.5%, 54.4%, and 60.5% for the C28, C30, and C32 homologues, respectively, are equivalent or in excess of mean soil carbonate values (37.6% to 55.0%) from the corresponding time interval reported by Fox et al (2012a).

While the two isotope records from biomarkers and carbonates are broadly

concordant, the reason for the wider range in *n*-alkanoic acid data relative to carbonates is not obvious. The difference is of particular interest for several reasons. First, the plant wax dataset (N=11) is much smaller than the corresponding soil carbonate dataset (N = >100), yet the plant waxes yield a greater range of $\%C_4$ vegetation. Second, very few studies have directly compared these two vegetation proxies, both of which are well-established and widely accepted. At present, the limited size of the plant wax dataset and lack of measurements from both proxies at the same stratigraphic level preclude a definitive explanation. Nevertheless, it is worth discussing possible reasons for the observed differences in $\%C_4$ vegetation.

The first and most likely explanation is that although sampled from the same stratigraphic interval, plant wax and carbonate samples do not actually represent the same point in time. For example, the three lowest $\%C_4$ values for biomarker samples come from two sites where there are no soil carbonates in the sediments. Both sites, XITB and Rexroad Loc. 3, are faunal sites (Fig. 2) and therefore were prioritized because of the opportunity to link paleoecological information to the faunal assemblages. Abundant charcoal was found at both sites in clay-rich sediments. In layers where charcoal was found, bedding is generally massive and structureless; however, rare laminations are preserved at Rexroad Loc. 3. There is no evidence of pedogenesis at either site. Charcoal from both sites is found in silty clays that were likely deposited in seasonally wet, lowland areas (e.g., ponds) or possibly floodplains. Detailed study of Meade Basin charcoal layers has just begun, but associated plant waxes from charcoal-bearing sediments yielded the most negative $\delta^{13}C$ values of all analyzed samples and low $\%C_4$ values (Table 1), suggesting some variation in vegetation structure between sections with and without carbonates.

A second explanation requires consideration of how soil carbonate and plant waxes may differ as paleovegetation proxies. The long chain (C28 to C32) *n*-alkanoic acids analyzed are actual remains of plants that are preserved in sediments. They are presumably derived from in situ production, yet there may be some contribution from plant waxes associated with aeolian dust or fluvial sediments transported into the basin. Analyses of plant-wax concentrations and $\delta^{13}C$ as a function of depth in the soil in modern Meade Basin soils and in well-preserved paleosols will address the question of biomarker inheritance in the Neogene sediments.

The $\delta^{13}C$ value of pedogenic carbonate precipitated from soil-respired CO_2 reflects vegetation type and although not plant material itself, the carbonate is directly linked to vegetation type under the right conditions (for a detailed review of the systematics see Fox et al., 2012b). Soil carbonates are limited to semi-arid and arid climates or places where PET is high. Carbonate precipitation occurs seasonally when soils are dewatered such that carbonate saturation conditions are met, which is likely driven by soil water evaporation or when plant uptake of water leads to exclusion of calcium and carbonate ions (Breecker et al., 2009; Quade et al., 2013). Climatological conditions associated with soil carbonate formation in the Meade Basin may also be associated with certain vegetation distributions and therefore may not capture the full range of ecosystems that existed in the past. Another dimension of the projects is reconstructing soil temperatures using clumped isotope thermometry, which will ultimately allow for reconstruction of MAT. To this end, soil temperature and moisture are being measure at three different sites in the basin. These modern data will provide insight on how to interpret clumped isotope data from Neogene carbonates in the basin, and on soil carbonate formation.

There are many unanswered questions related to the systematics of carbon isotopes in plant wax (*n*-alkane and *n*-alkanoic acids) and soil carbonates that may account for the observed differences in the Meade Basin plant wax and carbonate data. Efforts are currently underway to improve our understanding of these proxies. Our project in the Meade Basin offers a unique opportunity to delve into the different proxy systems because of the co-occurrence of plant waxes and carbonates in the sediments. The study of modern soils in the basin includes the soil temperature and moisture profiles discussed above, with additional carbon isotope data from plant waxes, soil organic matter, and carbonates planned. For the Neogene sediments, we are measuring carbon isotopes in plant waxes, carbonates, and bulk soil organic matter from the same stratigraphic level to directly compare the vegetation signal recorded in each proxy. We are also measuring carbon isotope ratios from plant wax and bulk organic matter occluded in large (stage II) carbonate nodules to further understand

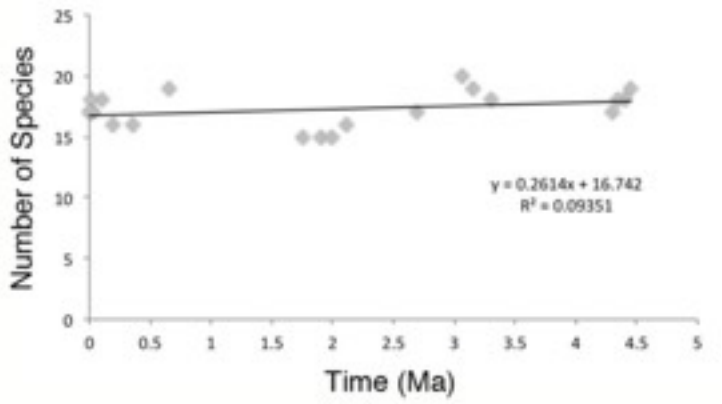

FIGURE *6*.—Species richness of Meade Basin rodent community as a function of time. Ma, millions of years ago.

carbon isotope systematics.

FAUNAL DYNAMICS OF MEADE BASIN RODENTS

In order to develop a biologically realistic and temporally controlled database of species occurrences in the Meade Basin, it was necessary to rediscover and recollect Hibbard's original localities, and to prospect for new fossiliferous levels to fill in gaps in Hibbard's original faunal succession. This process took many years, in part because it became clear that some previous stratigraphic assumptions were likely in error, and the outcrops had to be remapped. A number of gravels in the Meade Basin of different ages had in the past been considered coeval, and it took considerable time to decipher their correct stratigraphic positions and the stratigraphic positions of the rodent assemblages associated with them (e.g., Honey et al., 2005).

Species-level taxonomy of the Meade Basin rodents was re-examined, and various corrections were made (for the current form of the rodent database, please see the Appendix). Study continues as of this writing, and although the number of species in the database is likely near to a final tally, the taxonomy may undergo further minor modifications, particularly among sciurids and cricetines. The combination of field and lab work to date has only recently allowed beginning the series of analyses for which the database was originally intended. Below, we briefly summarize the current status of ecological studies of the Meade Basin rodents.

Our studies of the Meade Basin record of rodents confirm that species richness does not vary much (Fig. 6), and taxonomic turnover was relatively continuous throughout the 5 Myr period sampled by the MBRP (Martin and Fairbanks, 1999; Martin and Peláez-Campomanes, 2014), and that even major shifts from C_3 to C_4 plant communities (Martin et al., 2008; Fox et al., 2012a) do not shock the system into a new configuration. However, Martin and Peláez-Campomanes (2014) also identified relatively rapid spikes of extinction and immigration, apparently correlated with glacial intervals, and, at least in one case, with deposition of the Huckleberry Ridge ash at 2.11 Ma from the Yellowstone caldera. Deposition of the Huckleberry Ridge ash in particular appears to have had a direct impact on rodent community structure. The rich Borchers rodent assemblage (Hibbard, 1941) is developed within and directly on top of the ash. This assemblage includes the last record of the diminutive cotton rat *Sigmodon minor*, a species that characterizes Pliocene deposits in the basin. Thousands of cotton-rat specimens are known from Borchers. In the same set of outcrops, somewhat less than 2 meters above the ash, the Short Haul site preserves a decidedly different assemblage, including the first record of Holarctic *Microtus* in North America. Forty percent of the rodent species turn over during this interval. Additional specimens collected from Short Haul during field work in 2014 demonstrated the presence of a dwarf population of pocket gopher (*Geomys*). Because the pocket gopher record is the densest for any rodent group in the Meade Basin, we should be able to test if the Huckleberry Ridge ash drove this dwarfing. The apparent effects of the Huckleberry Ridge ash on community structure and, possibly, body-size evolution of at least one lineage of geomyid, suggest an important role for abiotic factors in the evolution of the Meade Basin rodent assemblage.

Recent analyses of modern species extinctions by Barnosky et al. (2011) have led to the prediction of a 'sixth mass extinction' based on estimates of current extinction rates that are an order of magnitude higher than those documented in the deep-time fossil record. Following Barnosky et al. (2011), and using a rate metric developed by Pimm et al. (1995, 2006), Martin and Peláez-Campomanes (2014) calculated extinction rates for 18 periods of varying length through the 5-million year Meade Basin rodent record. After removing extinction estimates for intervals of very short or uncertain duration, a relatively low background rate of 0–1(species extinctions)/million species-years (MSY) prevailed for most of the study period in the Meade Basin record, punctuated by higher levels at certain time periods. The two highest rates, 2.84/MSY and 1.40/MSY, correspond to community transitions following deposition of the Huckleberry Ridge and Lava Creek B ashfalls, the latter also from the Yellowstone caldera at 0.64 Ma. The extinction rates for modern species reported by Barnosky et al. (2011) range from 10–100/MSY. The Meade Basin record demonstrates that when sampling is dense at the species level, turnover patterns (and thus extinction rates) are not monotonic, and cannot be modeled appropriately by estimating average rates over long time intervals and wide geographic ranges. The MBRP record provides a critical comparison of mammalian background extinction rates for communities that include extant genera and species with modern species losses, and shows that, in agreement with Barnosky et al. (2011), mammalian extinction rates in the fossil record do not approach those for modern mammals due to anthropogenic activities.

Preliminary work on body-size distributions among Meade Basin rodent assemblages identified both problems and promising avenues of investigation. Martin (1996) generated body-mass estimates for the early Pliocene Fox Canyon rodent assemblage based on regressions of tooth size and body mass of modern species, then compared the size distributions in the Fox Canyon size hierarchy with that of the modern Meade County, Kansas, rodent community. Hutchinsonian ratios (Hutchinson, 1959) were calculated for contiguous size categories. Rather than finding significant separation of all size classes, in both the modern and Fox Canyon rodent assemblages, there were a number of potentially competitive species pairs that overlapped in size, leading to the speculation that competition could be operable. However, it is equally probable (one of the problems identified) that the species pairs were segregated through microhabitat selection; i.e., habitat heterogeneity (complexity) minimized competitive encounters. It will be difficult to determine which process dominated, but this is where stable isotopes and 3-D dental morphology may be helpful in determining specific diets for species with similar body sizes.

Of equal interest is the observation that certain size categories in the Fox Canyon rodent assemblage were unfilled in the modern community, and vice versa. We will generate size distributions for all Meade Basin rodent assemblages, and comparison of the distributions may reveal assembly rules for the Mead Basin community over time. Finally, using appropriate equations relating body mass to other physiological, behavioral, and life-history parameters (e.g., metabolic rate, home-range size, population density; Martin, 1986), we will generate estimates that will further identify tendencies among species that might have been both beneficial and detrimental to their long-term success.

CONCLUSIONS

With current sampling density through the interval of ca. 4–1 Ma, paleoenvironmental proxies from the Meade Basin suggest no clear patterns of short-term variability and no long-term trends in climatic conditions in the Meade Basin. The different proxies for MAP give different absolute values but maintain their relative ranking in terms of which gives the highest (CIA-K) and lowest (rock magnetics) estimates through the entire record. The C index for modern soils suggests it may be the most accurate in this system, which is not necessarily surprising given the carbon isotope evidence for abundant C_4 grasses throughout the Plio–Pleistocene record (Fox et al., 2012a). Estimates of MAP from the C index are generally close to the modern value of MAP for Meade, KS. We find that Δ_{47} temperature estimates were also relatively invariant throughout the interval, while $\delta^{18}O_w$ values (and percent C_4 plant biomass) increased through time. These results suggest that paleotemperature was either decoupled from paleohydrology and not a primary environmental factor responsible for changes in paleovegetation

and fauna in the Meade Basin, or that sampling density within and among measured sections is not sufficient to detect very short-term and rapid climatic shifts that could be driving turnover.

The $\delta^{13}C$ values of *n*-alkanoic acids from Neogene sediments record highly variable landscapes in terms of local dominant vegetation type that ranged from ~15% to 86% C_4 vegetation. Over the intervals sampled, there was no observable temporal trend in the *n*-alkanoic acids that indicated an expansion of C_4 vegetation as recorded in the paleosol carbonates. It is noteworthy that the two charcoal-bearing sites, XIT B and Rexroad Loc. 3, were C_3-dominated environments. These fossil localities were likely mesic environments with surrounding trees and other larger shrubby vegetation, as is commonly found today in southwestern Kansas around large collapse-basin springs in otherwise semi-arid prairie environments. This is supported to some extent by the recovery of giant beaver remains (*Procastoroides)* from Rexroad Loc. 3, indicating the presence of a significant body of water.

Overall, the absence of either long- or short-term variability in climate proxies might suggest that environmental change was not the primary driver of rodent community turnover. However, Holbrook's (1977) studies of rodent assemblages in archaeological time showed that levels of faunal shifts equivalent to the Meade Basin background turnover rate occur as a result of very brief environmental changes consistent with the equivalent of current prolonged droughts, although Holbrook was also careful to indicate that she was unable to eliminate competition as an influence. The long-term changes in the Meade Basin rodent record are consistent with environmental change at the beginning of the Pleistocene, resulting in loss of archaic arvicolids with rooted molars (*Ogmodontomys, Ophiomys*) and some cricetid species with ties to Central America and Mexico (e.g., small species of *Sigmodon*, *Bensonomys*), and gains in species more commonly encountered in global Holarctic environments, such as the arhizodont arvicolids *Microtus* and *Mictomys* (Martin et al., 2008). It is difficult to conclude that environmental change was not involved in this faunal succession, especially since *Microtus* dispersed from Siberia across the Beringian land bridge when sea level was low ca. 2.0 Ma (Martin et al., 2008). Rapid, basically geologically instantaneous, pulses of enhanced turnover following the Huckleberry Ridge ashfall also identifies environmental change as a likely forcing mechanism for rodent community change. These observations suggest that our geochemical climatic proxies faithfully record certain large-scale environmental patterns, such as the gradual shift in proportion of C_3 and C_4 grasses, but are currently unable to identify short-term stochastic environmental events that could drive community turnover. Denser sampling in important faunal intervals may be the key to identifying times of rapid and ecologically important environmental and/or climatic change that are not yet evident in our proxy records.

ACKNOWLEDGMENTS

This work would not have been possible without the generous access to outcrops provided by numerous land owners in and around Meade, KS. This research was funded by grants from the U.S. National Science Foundation Sedimentary Geology Program to Fox (EAR-0207383) and Martin (EAR-0207582) and from the Earth-Life Transitions (ELT) program to Fox (EAR-1338262, Fox-Dobbs (EAR-1338313), Snell (and J. Eiler; EAR-1338261), and Polissar and Uno (EAR- 1338243). We thank Jason Head for a helpful and thoughtful review.

REFERENCES

Alroy, J., P. L. Koch, and J. C. Zachos. 2000. Global climate change and North American mammalian evolution. Paleobiology, 26:259–288.

Affek, H. P. 2012. Clumped isotope paleothermometry: Principles, applications, and challenges, p. 101–114. *In* L. C. Ivany and B. Huber (eds.), Reconstructing Earth's Deep-Time Climate–The State of the Art in 2012. Paleontological Society Papers, 18.

Barnosky, A. D. 2001. Distinguishing the effects of the Red Queen and Court Jester on Miocene mammal evolution in the Northern Rocky Mountains. Journal of Vertebrate Paleontology, 21:172–185.

Barnosky, A. D., N. Matzke, S. Tomiya, G. O. U. Wogan, B. Swartz, T. B. Quental, C. Marshall, J. L. McGuire, E. L. Lindsey, K. C. Maguire, B. Mersey, and E. A. Ferrer. 2011. Has the Earth's sixth mass extinction arrived? Nature, 471:51–57.

Barry, J. C., M. E. Morgan, L. J. Flynn, D. Pilbeam, L. L. Jacobs, E. H. Lindsay, S. Mahmood Raza, and N. Solounias. 1995. Patterns of faunal turnover and diversity in the Neogene Siwaliks of northern Pakistan. Palaeogeography, Palaeoclimatology and Paleaoecology, 115:209–226

Breecker, D. O., Z. D. Sharp, and L. D. McFadden. 2009. Seasonal bias in the formation and stable

isotopic composition of pedogenic carbonate in modern soils from central New Mexico, USA. Geological Society of America Bulletin, 121:630–640.

Brett, C. E., and G. C. Baird. 1995. Coordinated stasis and evolutionary ecology of Silurian to middle Devonian faunas in the Appalachian Basin, p. 285–315. *In* D. H. Erwin and R. L. Anstey (eds.), New Approaches to Speciation in the Fossil Record. Columbia University Press, New York.

Burgoyne, T. W., and J. M. Hayes. 1998. Quantitative production of H2 by pyrolysis of gas chromatographic effluents. Analytical Chemistry, 70:5136–5141

Castañeda, I. S., J. P. Werne, T. C. Johnson, and T. R. Filley. 2009. Late Quaternary vegetation history of southeast Africa: the molecular isotopic record from Lake Malawi. Palaeogeography, Palaeoclimatology, Palaeoecology, 275:100–112.

Eglinton, G., and R. J. Hamilton. 1967. Leaf epicuticular waxes. Science, 156:1322–1335.

Eiler, J. M. 2007. "Clumped-isotope" geochemistry—The study of naturally-occurring, multiply-substituted isotopologues. Earth and Planetary Science Letters, 262:309–327.

Eiler, J. M., and E. Schauble. 2004. $^{13}C^{18}O^{16}O$ in Earth's atmosphere. Geochimica Et Cosmochimica Acta, 68:4767–4777.

Feakins, S. J., N. E. Levin, H. M. Liddy, A. Sieracki, T. I. Eglinton, and R. Bonnefille. 2013. Northeast African vegetation change over 12 my. Geology, 41:295–298.

Finarelli, J. A., and C. Badgley. 2010. Diversity dynamics of Miocene mammals in relation to the history of tectonism and climate. Proceedings of the Royal Society B-Biological Sciences,1098:1–6.

Fox, D. L, and P. L. Koch. 2003. Tertiary history of C_4 biomass in the Great Plains, U.S.A. Geology, 31:809–812.

Fox, D. L., and P. L. Koch. 2004. Carbon and oxygen isotopic variability in Neogene paleosol carbonates: constraints on the evolution of the C_4-dominated grasslands of the Great Plains, USA. Palaeogeography, Palaeoclimatology, Palaeoecology, 207:305–329.

Fox, D. L., J. G. Honey, R. A. Martin, and P. Peláez-Campomanes. 2012a. Pedogenic carbonate stable isotope record of environmental change during the Neogene in the southern Great Plains, southwest Kansas, USA: Oxygen isotopes and paleoclimate during the evolution of C_4-dominated grasslands. Geological Society of America Bulletin, 124:431–443.

Fox, D. L., J. G. Honey, R. A. Martin, and P. Peláez-Campomanes. 2012b. Pedogenic carbonate stable isotope record of environmental change during the Neogene in the southern Great Plains, southwest Kansas, USA: Carbon isotopes and the evolution of C_4-dominated grasslands, Geological Society of America Bulletin, 124:444–462.

Freeman, K. H., and L. A. Colarusso. 2001. Molecular and isotopic records of C4 grassland expansion in the late Miocene. Geochimica et Cosmochimica Acta, 65:1439–1454.

Geiss, C. E., R. Egli, and C. W. Zanner. 2008. Direct estimates of pedogenic magnetite as a tool to reconstruct past climates from buried soils. Journal of Geophysical Research, 113. doi: 10.1029/2008JB005669.

Ghosh, P., J. Adkins, H. Affek, B. Balta, W. F. Guo, E. A. Schauble, D. Schrag, and J. M. Eiler. 2006. ^{13}C–^{18}O bonds in carbonate minerals: A new kind of paleothermometer. Geochimica et Cosmochimica Acta, 70:1439–1456.

Hayes, J. M., K. H. Freeman, B. N. Popp, and C. H. Hoham. 1990. Compound-specific isotopic analyses; a novel tool for reconstruction of ancient biogeochemical processes. Organic Geochemistry, 16:1115–1128.

Heslop, D., and A. P. Roberts. 2013. Calculating uncertainties on predictions of palaeoprecipitation from the magnetic properties of soils. Global and Planetary Change, 110:379–385. doi:10.1016/j.gloplacha.2012.11.013.

Honey, J. G., P. Peláez-Campomanes, and R. A. Martin. 2005. Stratigraphic framework of early Pliocene localities along the north bank of the Cimarron River, Meade County, Kansas. Ameghiniana, 42:461–472.

Hibbard, C. W. 1941. The Borchers Fauna, a new Pleistocene interglacial fauna from Meade County, Kansas. Transactions of the Kansas Academy of Sciences, 40:239–265.

Hibbard, C. W., and D. W. Taylor. 1960. Two late Pleistocene faunas from southwestern Kansas. Contributions of the Museum of Paleontology, University of Michigan, 56:1–223.

Holbrook, S. J. 1977. Rodent faunal turnover and prehistoric community stability in northwestern New Mexico. American Naturalist, 111:1195–1208.

Hough, B. G., F. Fan, and B. H. Passey. 2014. Calibration of the clumped isotope geothermometer in soul carbonate in Wyoming and Nebraska, USA: Implications for paleoelevation and paleoclimatic reconstruction. Earth and Planetary Science Letters, 391:110–120.

Huntington, K. W., J. M. Eiler, H. P. Affek, W. Guo, M. Bonifacie, L. Y. Yeung, N. Thiagarajan, B. Passey, A. Tripati, M. Daeron, and R. Came. 2009. Methods and limitations of 'clumped' CO_2 isotope $\Delta 47$ analysis by gas-source isotope ratio mass spectrometry. Journal of Mass Spectrometry, 44:1318–1329.

Hutchinson, G. E. 1959. Homage to Santa Rosalia, or

why are there so many kinds of animals. American Naturalist, 93:145–259.
Izett, G. A., and J. G. Honey. 1995. Geologic map of the Irish Flats NE quadrangle, Meade County, Kansas. United States Geological Survey Miscellaneous Investigations Series Map I-2498, 1:24,000.
Jaeger, R. G. 1974. Competitive exclusions: comments on survival and extinction of species. BioScience, 24:33–39.
MacArthur, R. H., and E. O. Wilson. 1967. The Theory of Island Biogeography. Princeton University Press, Princeton, N. J.
Martin, R. A. 1986. Energy, ecology and cotton rat evolution. Paleobiology, 12:370–382.
Martin, R. A. 1996. Tracking mammal body size distributions in the fossil record: a preliminary test of the 'rule of limiting similarity.' Acta Zoologica Cracoviensia, 39:321–328.
Martin, R. A., and K. B. Fairbanks. 1999. Cohesion and survivorship of a rodent community during the past 4 million years in southwestern Kansas. Evolutionary Ecology Research, 1:21–48.
Martin, R. A., and P. Peláez-Campomanes. 2014. Diversity dynamics of the Late Cenozoic rodent community from south-western Kansas: the influence of historical processes on community structure. Journal of Quaternary Science, 29:221–231.
Martin, R. A., P. Peláez-Campomanes, and J. G. Honey. 2000. The Meade Basin rodent project: a progress report. Paludicola, 3:1–32.
Martin, R. A., P. Peláez-Campomanes, and C. Mecklin. 2012. Patterns of size change in late Neogene pocket gophers from the Meade Basin of Kansas and Oklahoma. Historical Biology, 24:537–545.
Martin, R. A., P. Peláez-Campomanes, J. G. Honey, D. L. Fox, R. J. Zakrzewski, L. B. Albright, E. H. Lindsay, N. D. Opdyke, and H. T. Goodwin. 2008. Rodent community change at the Pliocene–Pleistocene transition in southwestern Kansas and identification of the *Microtus* immigration event on the Central Great Plains. Palaeogeography, Palaeoclimatology, Palaeoecology, 267:196–207.
Mccune, A. R. 1982. On the fallacy of constant extinction rates. Evolution, 36:610–614.
Passey, B. H., N. E. Levin, T. E. Cerling, F. H. Brown, and J. M. Eiler. 2010. High-temperature environments of human evolution in East Africa based on bond ordering in paleosol carbonates. Proceedings of the National Academy of Sciences of the United States of America, 107:11245–11249.
Pimm, S. L., G. J. Russell, J. L. Gittleman, and T. M. Brooks. 1995. The future of biodiversity. Science, 269:347–350.
Pimm, S. L., P. Raven, A. Peterson, Ç. H.Şekercioğlu, and P. R. Ehrlich. 2006. Human impacts on the rates of recent, present and future bird extinctions. Proceedings of the National Academy of Science, 103:10941–10946.
Polissar, P. J., K. H. Freeman, D. B. Rowley, F. A. McInerney, and B. S. Currie. 2009. Paleoaltimetry of the Tibetan Plateau from D/H ratios of lipid biomarkers. Earth and Planetary Science Letters, 287:64–76.
Quade, J., J. Eiler, M. Daëron, and H. Achyuthan. 2013. The clumped isotope geothermometer in soil and paleosol carbonate. Geochimica Et Cosmochimica Acta, 105:92–107.
Retallack, G. J. 2007. Cenozoic paleoclimate on land in North America. The Journal of Geology, 115:271–294. doi: 10.1086/512753.
Sheldon, N. D., and N. J. Tabor. 2009. Quantitative paleoenvironmental and paleoclimatic reconstruction using paleosols. Earth-Science Reviews, 95:1–52. doi:10.1016/j.earscirev.2009.03.004.
Sheldon, N. D., G. J. Retallack, and S. Tanaka. 2002. Geochemical climofunctions from North American soils and application to paleosols across the Eocene–Oligocene boundary in Oregon. Journal of Geology, 110:687–696.
Smith, F. A., S. L. Wing, and K. H. Freeman. 2007. Magnitude of the carbon isotope excursion at the Paleocene–Eocene thermal maximum: the role of plant community change. Earth and Planetary Science Letters, 262:50–65.
Snell, K. E., P. L. Koch, P. Druschke, B. Z. Foreman, and J. M. Eiler. 2013. High elevation of the 'Nevadaplano' during the Late Cretaceous. Earth and Planetary Science Letters, 386:52–63.
Swart, P. K., S. J. Burns, and J. J. Leder. 1991. Fractionation of the stable isotopes of oxygen and carbon in carbon dioxide during the reaction of calcite with phosphoric acid as a function of temperature and technique. Chemical Geology, 86:89–96.
Tipple, B. J., and M. Pagani. 2010. A 35 Myr North American leaf-wax compound-specific carbon and hydrogen isotope record: implications for C_4 grasslands and hydrologic cycle dynamics. Earth and Planetary Sciences Letters, 299:250–262.
van Valen, L. 1973. A new evolutionary law. Evolutionary Theory, 1:1–30.
Vrba, E. S. 1993. Turnover-pulses, the Red Queen, and related topics. American Journal of Science, 293-A:418–452.
Vrba, E. S. 1995. On the connections between paleoclimate and evolution, p. 24–45. *In* E. S. Vrba, G. H. Denton, T C. Partridge, and L. H. Burckle (eds.), Paleoclimate and Evolution, with Emphasis on Human Origins. Yale University Press, New Haven.
Wang, Z. G., E. A. Schauble, and J. M. Eiler. 2004. Equilibrium thermodynamics of multiply

substituted isotopologues of molecular gases. Geochimica et Cosmochimica Acta, 68:4779–4797.

Zakrzewski, R. J. 1975. Pleistocene stratigraphy and paleontology in western Kansas: the state of the art, 1974, p. 121–128. *In* G. R. Smith and N. E. Friedland (eds.), Studies on Cenozoic Paleontology and Stratigraphy in Honor of Claude W. Hibbard. University of Michigan, Papers on Paleontology 12.

APPENDIX Fox et al.

Rodent species recovered from selected local faunas from the Meade Basin of southwestern Kansas. SR/SR1, Sawrock Canyon/Saw Rock Canyon 1; Arg, Argonaut; FAB, Fallen Angel B; FC, Fox Canyon; RF, Red Fox; RipB, Ripley B; Rap1C, Raptor 1C; WnsB, Wiens B; Vas/Nwt, Vasquez/Newt; Hor, Hornet; RR3, Rexroad Loc. 3; DP, Deer Park A&B; Pal, Paloma; Ss, Sanders; Bor, Borchers; ArA, Aries A; Na72, Nash 72; RF, Rick Forester; Cud, Cudahy; Sun, Sunbrite; BS, Butler Spring; CQ, Cragin Quarry; Jin, Jinglebob; Jon, Jones; GolB, Golliher B; Rob, Robert; Mod, Modern; o, range-through taxon; ?, questionably present; K, in Kansas, but not Meade Basin.

	SR/SR1	Arg	FAB	FC	RFx	XIT1B	RipB	Rap1C	Wns	Vas/Nwt	Hor	RR3	DP	Pal	Ss	Bor	SH	ArA	Na72	RF	Cud	Sun	BS	CQ	Jin	Jon	GolB	Rob	Mod
Rodentia																													
Sciuridae																													
Paenemarmota barbouri /sawrockensis	x	o	o																										
Paenemarmota b. /barbouri				x	o	o	o	x																					
Ammospermophilus sp.						x																							
Otospermophilus rexroadensis				x	o	x	x	o	x	x	x	x	x																
Ictidomys howelli-meadensis				x	o	x	o	o	x	x	x	x	x	o	o	x													
Ictidomys tridecemlineatus																	x	x	x	o	x	o	x	x	x	x	x	x	x
Xerospermophilus spilosoma																													x
Poliocitellus lorisrusselli-franklini																					x				x	cf			
Urocitellus cragini																x													
Urocitellus richardsoni																					x	x	x			x	x	x	
Cynomys hibbardi-sappaensis																			x										
Cynomys spenceri-ludovicianus																							x						x
Cynomys niobrarius																							x	x					
Cynomys n. sp. (small)																						x							
Cynomys sp.																					o	x							
Uncertain ground squirrel							x			x				o	o		o	o									x		
Geomyidae																													
Pliogeomys louderbacki	x	x	x																										
Geomys adamsi				x																									
Geomys minor				x	o	x	x	o	x	x	x	x	x	?															
Geomys jacobi									cf	x	cf	x																	
Geomys quinni													x	?		x													
Geomys bursarius																				cf			cf	x	cf	x	cf	cf	x
Geomys tobinensis																					x	o							
Geomys floralindae															x	x													
Geomys n. sp.																	x	o	x										
Thomomys sp.																					x	o				x	x	x	
Heteromyidae																													
Prodipodomys sp.	x	o	o	x	o	?	x	x	x	o	o	x	x	o	x	x	o	o	x										
Dipodomys hibbardi																x													
Dipodomys ordii																							cf	cf	cf	o	o	o	x
Dipodomys sp.																				?	?	?							
Perognathus sp. 1	x	o	o	x	o	?	x	x	x	o	x	x	x	o	x	x	x	x	x	o	o	o	x	x	x	x	o	o	x
Perognathus sp. 2	x	o	o	x	o	?	o	o	o	o	o	o	o	o	o	o	o	o	x	o	o	o	o	o	x	o	o	o	x
Chaetodipus hispidus																							x	x	x	o	o	o	x
Cricetidae																													
Copemys sp.		cf	x																										
Symmetrodontomys simplicidens	x	x	x	x	x	cf	x	cf	cf	x	x	x	x	x															
Bensonomys stirtoni	x	x	x																										
Bensonomys arizonae				x	x	x	x	x	x	x	x	x	x	x															
Bensonomys meadensis															x														
Baiomys rexroadi	x	x	x	x	x	cf	x	x	x	cf	x	x																	
Baiomys minimus													x																
Onychomys leucogaster	x	x	x	x	x	x	x	x	x	x	x	x	x	o	o	x	x	x	x	o	x	o	x	x	x	x	x	x	x
Reithrodontomys wetmorei				x	o	cf	x	x	cf	o	cf	o	o	x															
Reithrodontomys moorei																x	x	x	x	o	x	o							
Reithrodontomys megalotis																							cf	cf					x
Reithrodontomys montanus																									cf				x
Reithrodontomys sp.																		x	x							o	x	x	
Peromyscus kansasensis												x	cf																
Peromyscus maniculatus																					cf	cf	o	cf	cf	cf			x
Peromyscus sp.						x					x									o							x	x	
Oryzomys palustris																									x				
Neotoma sawrockensis	x																												
Neotoma quadriplicata		o	o	x	o		x	o	x	o	x	x	x																
Neotoma taylori																x													
Neotoma micropus																								x	cf	o	o	o	x
Neotoma sp.						x								o	o		o	o	o	o	o	o	o						
Sigmodon holocuspis								x																					
Sigmodon minor		cf	cf				cf				x	x	x	x	x	x													
Sigmodon curtisi																	x	x											
Sigmodon hispidus																													x

APPENDIX, continued.

Rodent species recovered from selected local faunas from the Meade Basin of southwestern Kansas. SR/SR1, Sawrock Canyon/Saw Rock Canyon 1; Arg, Argonaut; FAB, Fallen Angel B; FC, Fox Canyon; RF, Red Fox; RipB, Ripley B; Rap1C, Raptor 1C; WnsB, Wiens B; Vas/Nwt, Vasquez/Newt; Hor, Hornet; RR3, Rexroad Loc. 3; DP, Deer Park A&B; Pal, Paloma; Ss, Sanders; Bor, Borchers; ArA, Aries A; Na72, Nash 72; RF, Rick Forester; Cud, Cudahy; Sun, Sunbrite; BS, Butler Spring; CQ, Cragin Quarry; Jin, Jinglebob; Jon, Jones; GolB, Golliher B; Rob, Robert; Mod, Modern; o, range-through taxon; ?, questionably present; K, in Kansas, but not Meade Basin.

	SR/SR1	Arg	FAB	FC	RFx	XIT1B	RipB	Rap1C	Wns	Vas/Nwt	Hor	R3	DP	Pal	Ss	Bor	SH	ArA	Na72	RF	Cud	Sun	BS	CQ	Jin	Jon	GolB	Rob	Mod
Arvicolidae																													
Ogmodontomys sawrockensis	x	x	x																										
Ogmodontomys poaphagus				x	x	x	x	x	x	x	x	x	x	x															
Pliophenacomys finneyi				x																									
Ophiomys meadensis															x														
Ptiolemmus antiguus													x	o	x														
Nebraskomys rexroadensis												x	x																
Mictomys landesi																x													
Mictomys kansasensis																	x	o	x	o									
Mictomys meltoni																					x	o							
Mictomys sp.																													
Synaptomys australis																									x				
Synaptomys cooperi																												x	x
Microtus pilocaenicus																	x	x	x	o									
Microtus paroperarius																					x	x							
Microtus meadensis																					x	x							
Microtus llanensis																					x	x							
Microtus ochrogaster																							x	cf	x	x			x
Microtus parmaleei																											x	cf	
Microtus pennsylvanicus																							x	x	x	x	x	x	K
Dipodidae																													
Zapus rinkeri				x	o																								
Zapus sandersi						o	o	o	o	o	cf	x	cf	o	x	o	o	o	o	o	cf	o							
Zapus hudsonius																							o	o	x	o		x	K
Zapus princeps																											x		